

Supporting Information

Carbon containing conductive networks in composite particle-based Photoanodes for Solar Watersplitting

Stefan Dilger,* Steve Landsmann, Matthias Trottmann, Simone Pokrant*

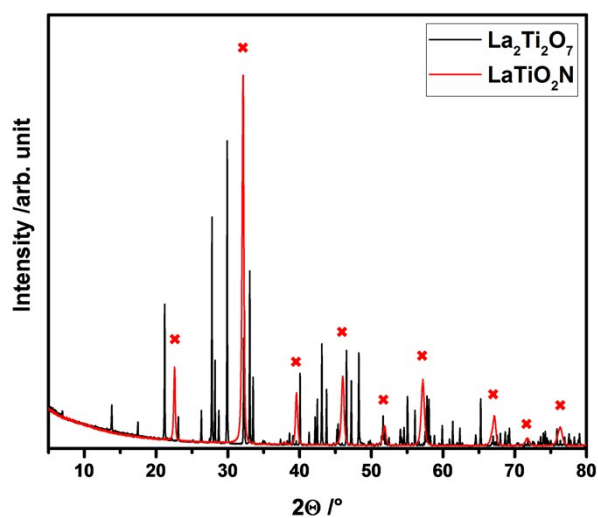


Figure SI 1. Powder x-ray diffractograms of $\text{La}_2\text{Ti}_2\text{O}_7$ (black line) and LaTiO_2N (red line). The red crosses indicate the reflections of the LaTiO_2N Imma phase.

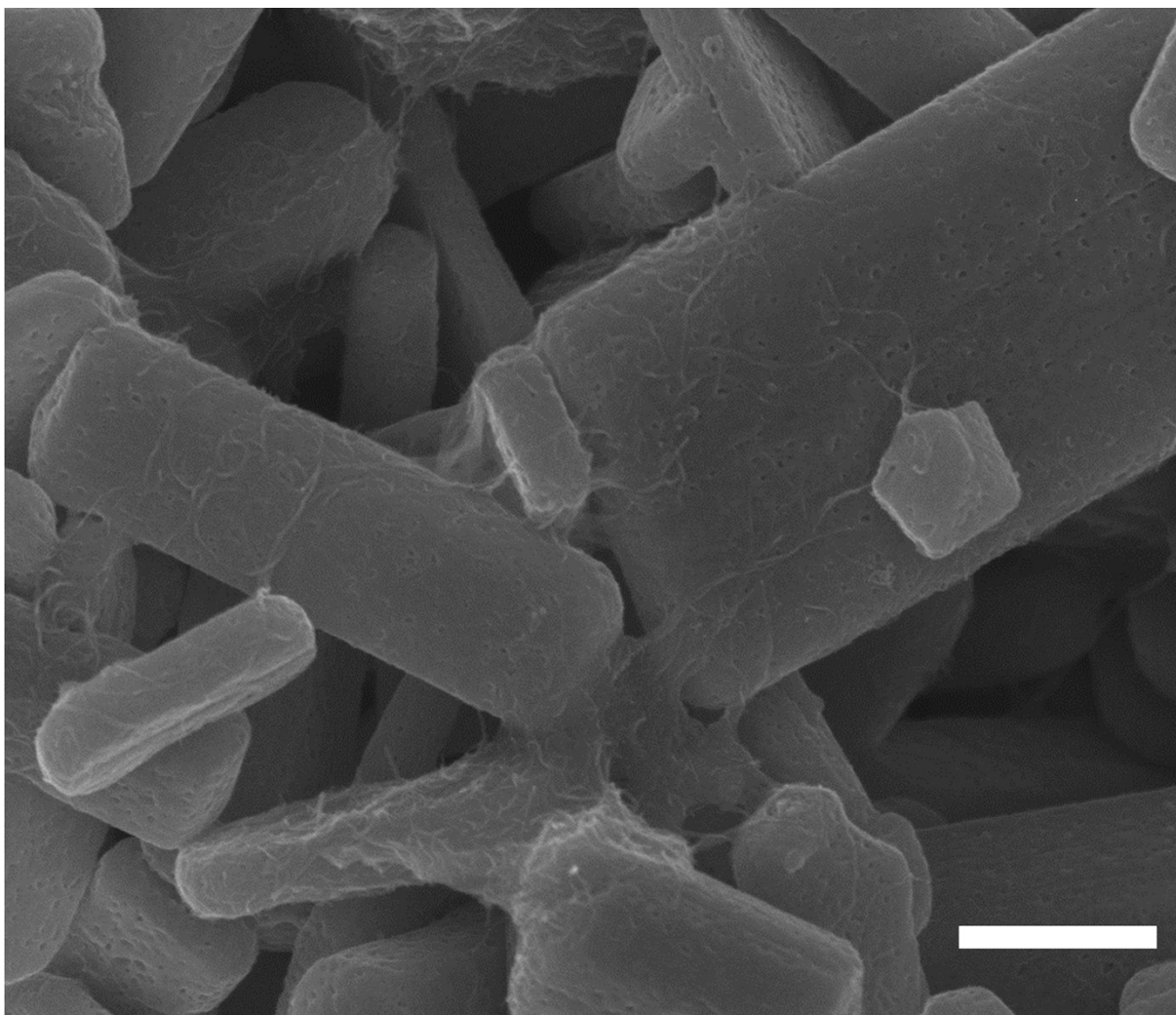


Figure SI 2. SEM image of hybrid composite electrode material with 1.0 wt% MWCNTs and 0.01 wt% GO on LTON.

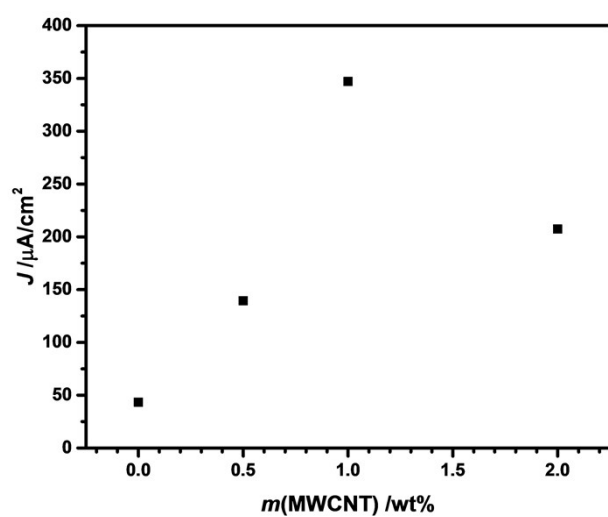


Figure SI 3. Photocurrent produced at 1.23 V vs. RHE under AM1.5G illumination by electrodes prepared with 2.0 min deposition times and varying MWCNT content. Photocurrent scans can be found in Figure SI 4.

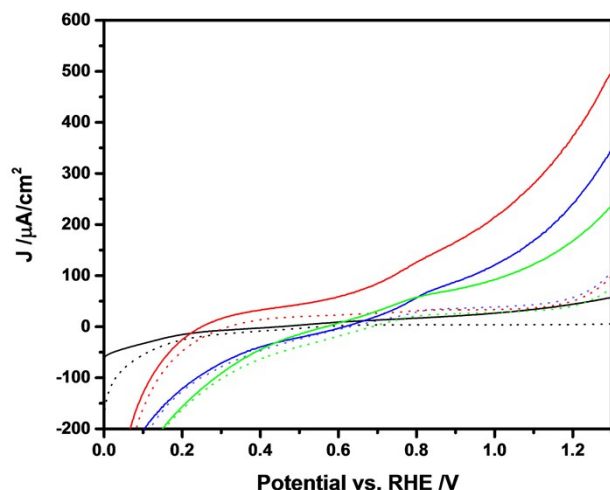


Figure SI 4. Photocurrent scans for Figure SI 3. Electrodes prepared with 2.0 min deposition time and varying MWCNT content.

Solid lines: Photocurrent measurements under AM1.5G back side illumination
Dotted lines: Measurements in the dark

Black: LTON
Green: + 0.5 wt% MWCNT
Red: + 1.0 wt% MWCNT
Blue: + 2.0 wt% MWCNT

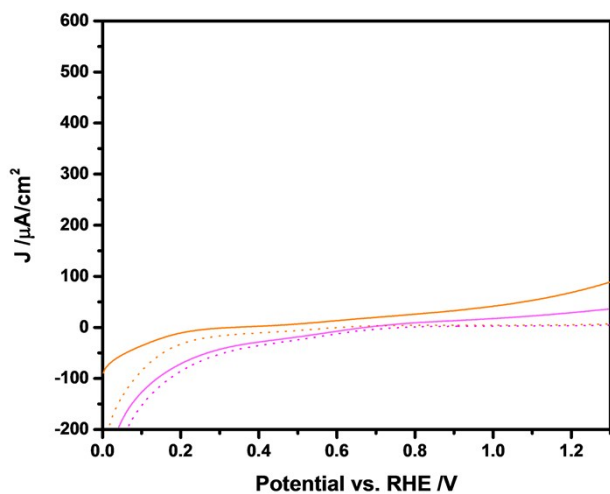


Figure SI 5. Photocurrent scans for electrodes prepared with 2.0 min deposition time and varying GO content

Solid lines: Photocurrent measurements under AM1.5G back side illumination
Dotted lines: Measurements in the dark

Orange: LTON + 0.01 wt% GO
Magenta: LTON + 0.05 wt% GO



Figure SI 6. Picture of destroyed electrode after measurement. This electrode's active material contained 1 wt% GO and no additional TiO₂ necking was applied to improve stability. The film lifted off the FTO slide and floated on the water during measurement, indicating a hydrophobic particle surface due to significant GO coverage.

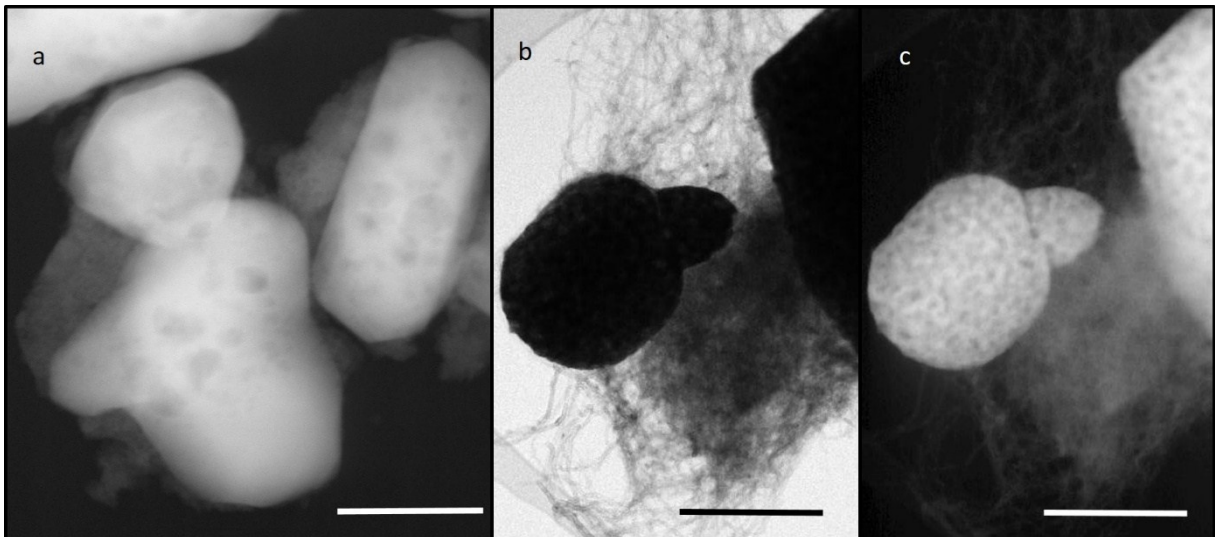


Figure SI 7. Scanning transmission electron images of a) LTON-Particles with TiO₂ necking, (dark field, scale bar 100 nm) b) LTON particles with TiO₂ necking and MWCNT (bright field, 500nm scale bar) c) LTON particles with TiO₂ necking and MWCNT (dark field, 500nm scale bar)

Figure SI 7a shows the localized TiO₂ connections induced by necking in pure LTON particles. The TiO₂ bridges (light grey, amorphous) are mainly localized at particle edges and interconnect particles at short distances (10-20 nm range). In the

presence of MWCNT the morphology of the TiO_2 necking changes significantly. In Figure SI 7b the MWCNT are clearly defined on the upper and lower part of the image, while on the right side a darker (thicker) area with badly defined structures dominates. Figure SI 7c shows that this thicker area consists of denser material. EDX analysis reveals the presences of TiO_2 . The same behaviour was found on other sites. TiO_2 deposits on MWCNTs in lumps reinforcing the MWCNT connections, while no short range TiO_2 bridges were observed.

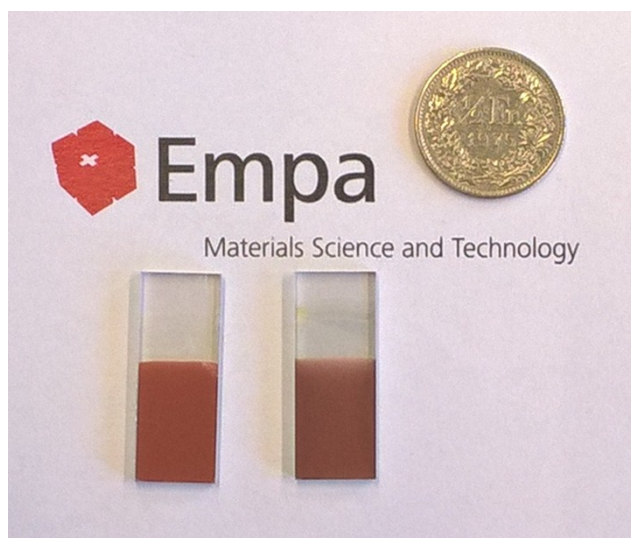


Figure SI 8. Photograph of LTON electrodes: LTON on the left, LTON + 1.0 wt% MWCNT on the right.

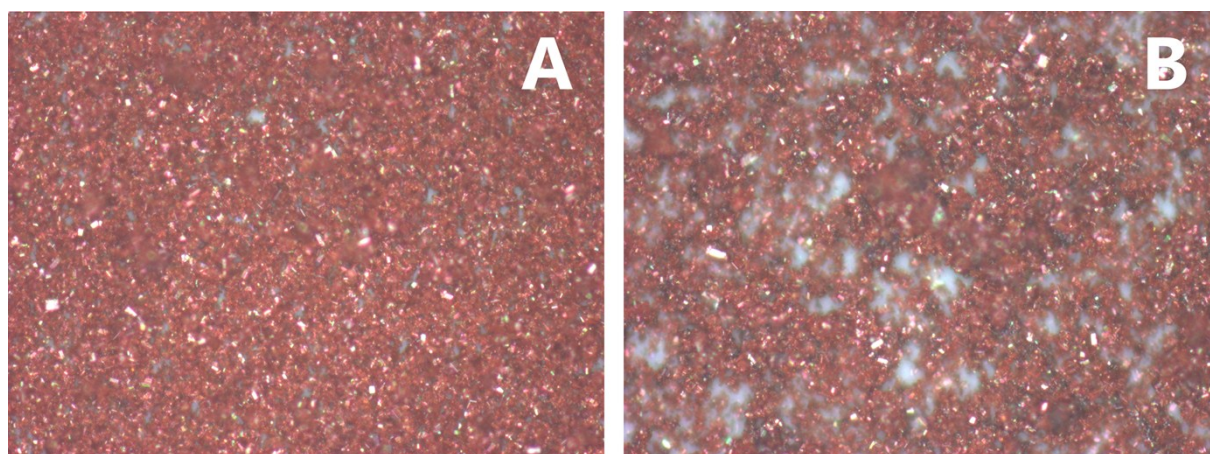


Figure SI 9. Optical Microscopy images at 20 x magnifications for electrodes prepared with different carbon content and 2.0 min deposition time. A: 0.01 wt% GO/LTON; B: 1.0 wt% of MWCNTs + 0.01 wt% GO/LTON.

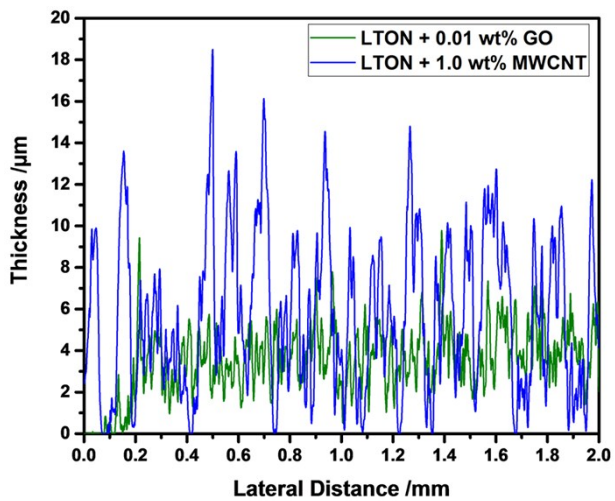


Figure SI 10. Profilometry data of electrodes with 0.01 wt% GO/LTON (green) and 1.0 wt% of MWCNTs/LTON (blue) visualising the different film roughnesses.

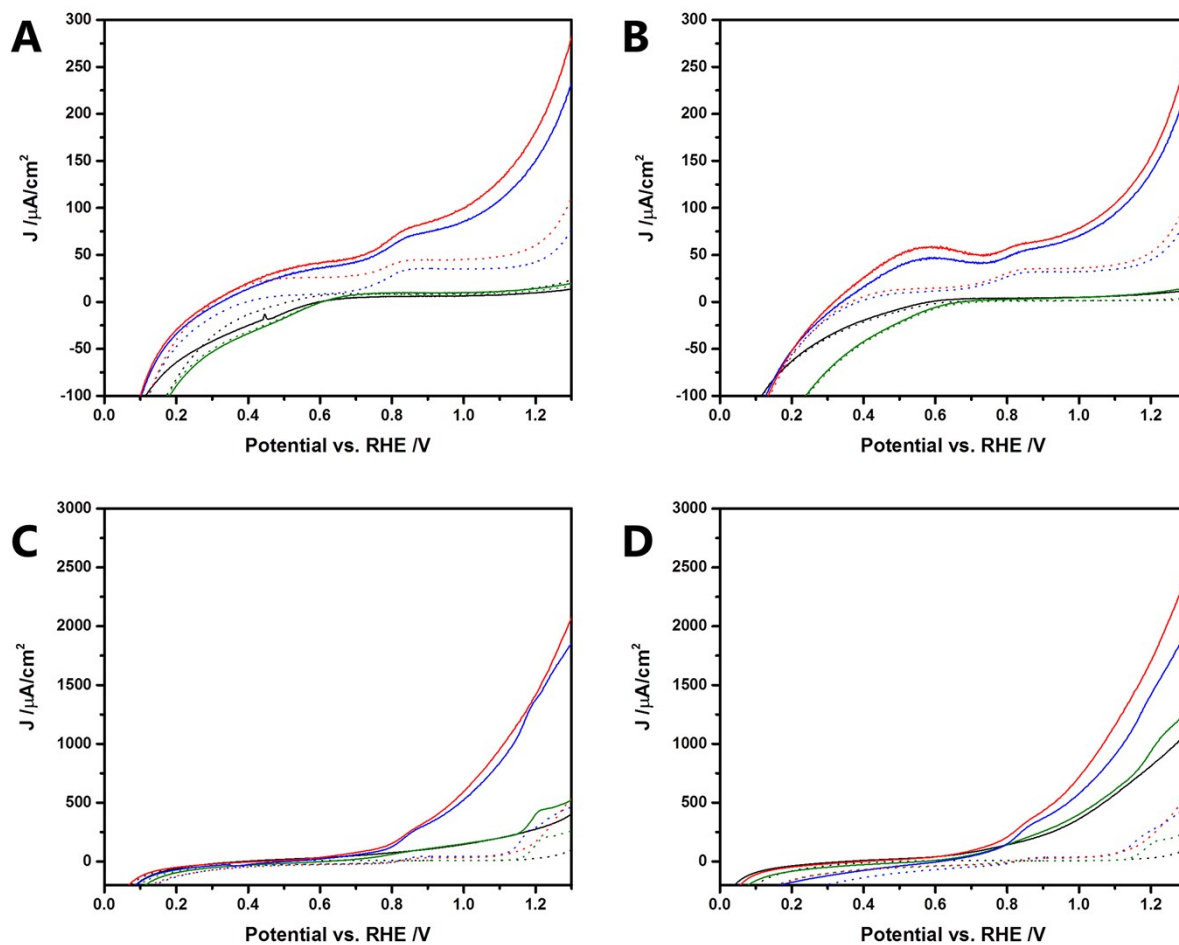


Figure SI 11. Photocurrent scans for Figure 5. Electrodes prepared with 2.0 min deposition time and varying MWCNT and GO content.

Solid lines: Photocurrent measurements under AM1.5G illumination
 Dotted lines: measurements in the dark

- A) Front side illumination, electrodes without co-catalysts
- B) Back side illumination, electrodes without co-catalysts
- C) Front side illumination, electrodes with co-catalysts
- D) Back side illumination, electrodes with co-catalysts

Black: LTON
 Green: + 0.01 wt% GO
 Blue: + 1wt% MWCNT
 Red: + 1 wt% MWCNT + 0.01 wt% GO

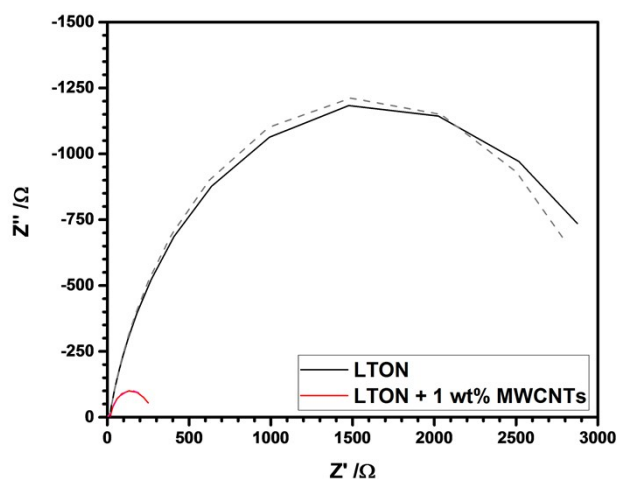
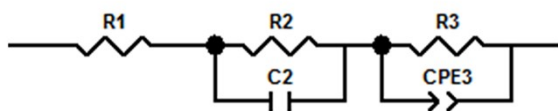


Figure SI 12. Electrochemical impedance data of LTON photoelectrodes under AM1.5G back illumination. Black curves: Pure LTON electrode, grey striped line: respective simulated data. Red curve: 1 wt% MWCNT containing LTON electrode, purple striped line: respective simulated data.

Electrochemical impedance measurements were carried out at 1.0 V vs. RHE using a Zahner IM6 with a 50 mV AC amplitude and a frequency range of 0.3 Hz – 1.0 MHz. An aqueous solution of 0.1 M Na_2SO_4 with pH 13.4 (NaOH) was used. An Ag/AgCl reference electrode (in 3 M KCl) and a Pt wire as counter electrode were used. A 300 W Xe lamp (Lot Oriel) equipped with an AM1.5G filter with an intensity of 100 mW/cm^2 calibrated with a Si photodiode was the light source. Data were analysed by simulations using ZView 2.80. The model used in and data obtained from the ZView fit are shown below. Most notably, a drop in resistance in the low frequency regime (R_3) as well as a frequency shift of the maximum of the low frequency semicircle to lower frequencies (higher CEP3-T) can be seen with the addition of MWCNT, indicative of lower resistances and higher charge carrier densities in the composite electrodes.



	• LTON	• LTON + MWCNT
• R_1 / Ω	• 4,198	• 5,806
• R_2 / Ω	• 9,431	• 11,53
• C_2 / F	• 1,80E-07	• 1,59E-07
• R_3 / Ω	• 3143	• 261,5
• CEP3-T / F	• 4,95E-05	• 6,76E-4
• CEP3-P	• 0,8379	• 0,84162

Model and analysis data from the EIS simulation in ZView

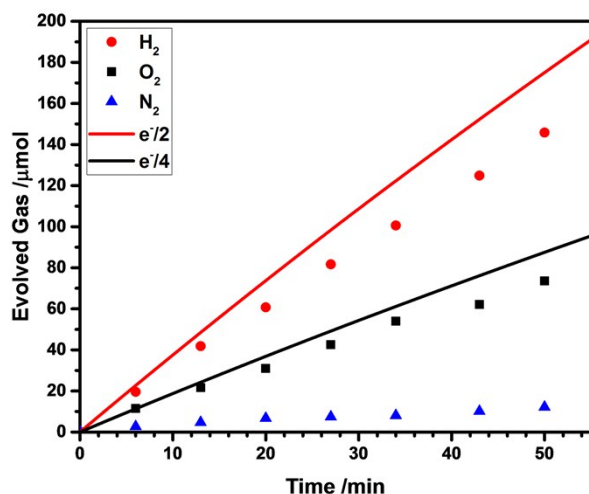


Figure SI 13. Gas evolution measurement under illumination of a 20cm² electrode area at 1.6 V vs. RHE for a co-catalyst containing electrode with 1.0 wt% MWCNT.

H₂: Red circles
 O₂: Black squares
 N₂: blue triangles

Gas chromatography measurements were performed to demonstrate gas evolution in the composite electrodes. Gas evolution was measured using an Inficon gas chromatograph attached to a three electrode custom built air tight cell with an Ag/AgCl reference electrode and a Pt spiral counter electrode. The gas chamber was evacuated and flushed with Ar ten times prior to measurement. An upscaled co-catalyst and 1.0 wt% MWCNT containing electrode with an AM 1.5 illuminated area of 20 cm² was used at 1.6 V vs RHE in an aqueous solution of 0.1 M Na₂SO₄ with pH 13.40 adjusted by adding NaOH. An H₂ to O₂ ration of 1.98 is obtained and the Faradaic efficiency was obtained as 83% and 84% for hydrogen and oxygen respectively, which is in agreement with literature results.^[1] For the photocurrent measurement see Figure SI 14.

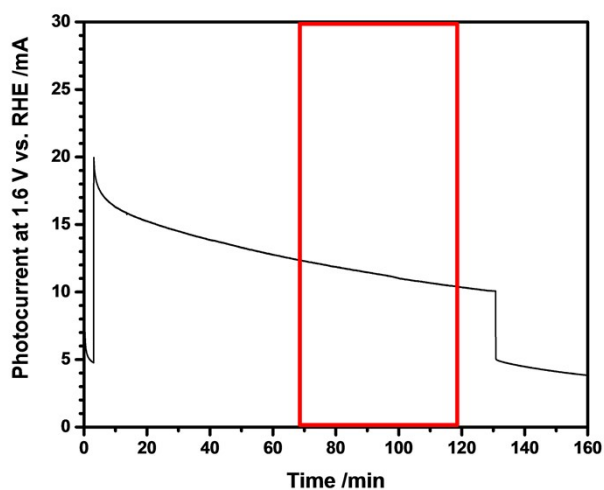


Figure SI 14. Photocurrent measurement for the GC experiment on the 20 cm² electrode shown in SI 13. Gas chromatography was measured after an equilibration period of 68 minutes, marked by the red rectangle. Please note, that lower current densities are expected when measuring gas evolution using large scale electrodes as discussed in ref^[1b].

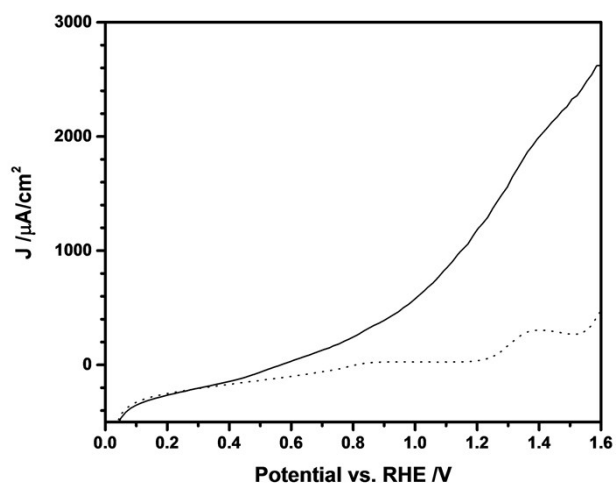


Figure SI 15. Photocurrent measurements up to 1.6 V vs. RHE in the dark (dotted line) and under 1.5 AM illumination in back configuration (black line) for a co-catalyst containing LTON electrode containing 0.5 wt% MWCNTs.

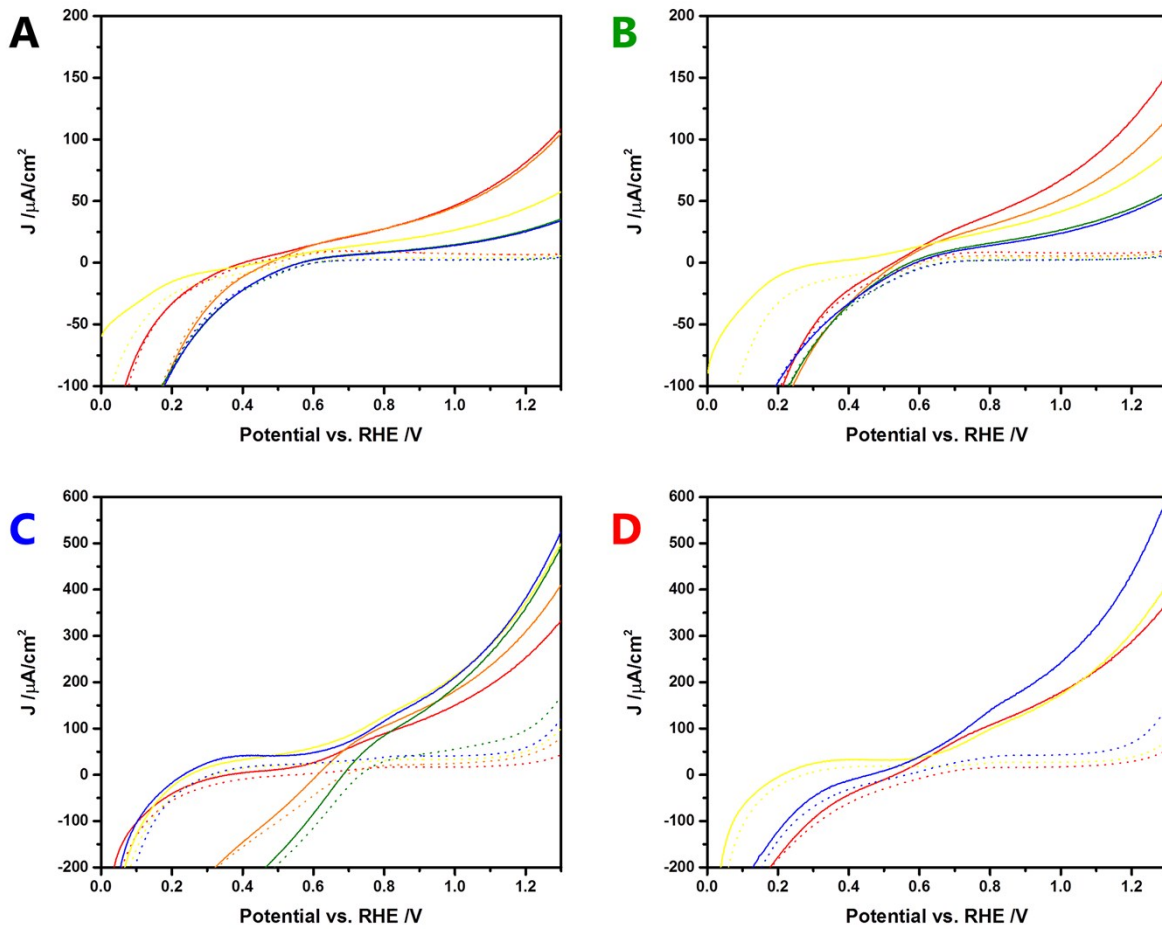


Figure SI 16. Photocurrent scans for Figure 6. Electrodes prepared with different deposition times.

Solid lines: Photocurrent measurements under AM1.5G back side illumination
Dotted lines: Measurements in the dark

Black A): LTON
Green B): + 0.01 wt% GO
Blue C): + 1.0 wt% MWCNT
Red D): + 1.0 wt% MWCNT + 0.01 wt% GO

Red lines: 30s
Orange lines: 60s
Yellow lines: 120s
Green lines: 180s
Blue lines: 240s

In some samples an increased potential for cathodic currents can be observed, due to electrode polarization during forward scan measurements. They are notably absent in cyclic voltammetric measurements starting from cycle 2, see Figure SI 17.

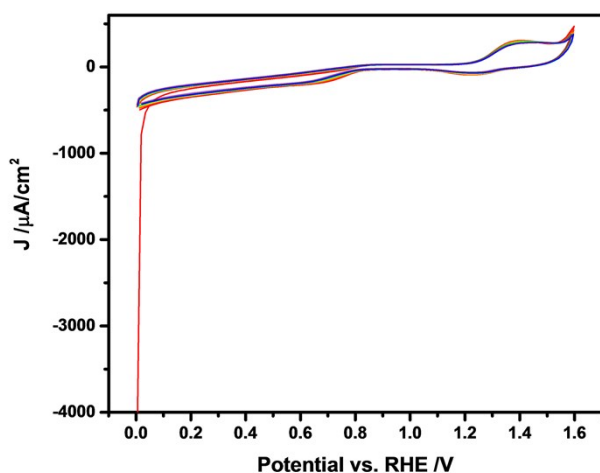


Figure SI 17. Cyclic voltammetric measurement of a co-catalyst containing electrode with 0.5 wt% MWCNTs in the dark. 10 cycles have been color coded by wavelength from red (first cycle) to violet (10th cycle). The peak at 0.7 V vs RHE is attributed to carbon oxide species present in the MWCNTs^[2]. The curve shape of the cyclic voltammetric measurements at voltages above 1.0 V vs. RHE has been discussed in the literature in ref^[3] and is attributed to co-catalyst effects.

[1] a) J. Y. Feng, W. J. Luo, T. Fang, H. Lv, Z. Q. Wang, J. Gao, W. M. Liu, T. Yu, Z. S. Li, Z. G. Zou, *Adv. Funct. Mater.* **2014**, 24, 3535; b) S. Haussener, C. Xiang, J. M. Spurgeon, S. Ardo, N. S. Lewis, A. Z. Weber, *Energ Environ Sci* **2012**, 5, 9922.

[2] a) Y. Shao, G. Yin, J. Zhang, Y. Gao, *Electrochim. Acta* **2006**, 51, 5853; b) J.-S. Ye, X. Liu, H. F. Cui, W.-D. Zhang, F.-S. Sheu, T. M. Lim, *Electrochem. Commun.* **2005**, 7, 249; c) J. J. Gooding, *Electrochim. Acta* **2005**, 50, 3049.

[3] S. Landsmann, Y. Surace, M. Trottmann, S. Dilger, A. Weidenkaff, S. Pokrant, *ACS Appl. Mater. Interfaces* **2016**, 8, 12149.